Transient Change Detection for LOS and NLOS Discrimination at GNSS Signal Processing Level

Daniel Egea-Roca, Gonzalo Seco-Granados, José A. López-Salcedo
Dpt. of Telecommunications and Systems Engineering, Universitat Autònoma de Barcelona (UAB), Spain

***Abstract*—Multipath is one of the major impairments threatening the integrity of terrestrial Global Navigation Satellite Systems (GNSS). For this reason, multipath mitigation has attracted the attention of many researchers, thus leading to outstanding contributions in the past years. These techniques are useful when the Line of Sight (LOS) is not obstructed. Otherwise, they are not applicable, and thus we should use alternatives exploiting Non-Line of Sight (NLOS) conditions. It is for this reason that the discrimination between LOS and NLOS situations may be beneficial for integrity in terrestrial GNSS applications. Several contributions for doing so have been proposed, but relying on external aid that is not often available in mass-market receivers. In this paper, we take a leap forward by adopting a transient change detection framework for discriminating between LOS and NLOS conditions. This is done by using the Slope Asymmetry Metric (SAM), which can be calculated within the GNSS receiver at the signal processing level, without using external aid, thus adequate for mass-market receivers. Numerical results will be used to validate the proposed solution, contributing to improve the GNSS integrity in terrestrial environments.**

I. Introduction

Nowadays, a plethora of Global Navigation Satellite Systems (GNSS) terrestrial-based liability- and safety-critical applications have appeared [1]. In these applications it is crucial to have the capability of providing timely warnings to the user when the system should not be used; this capability is referred to as the *integrity* of the system. To do so in terrestrial environments, it is of paramount importance to promptly detect any possible anomaly or misleading behavior that could be endangering the received GNSS signal [2]; we refer to this capability as the *signal integrity*.

In this paper, we focus on multipath as the major impairment that can threat the signal integrity of GNSS in urban environments. In the past decades, the detection of multipath has attracted the attention of many researchers. Multipath can be clasifie as Line-of-Sight (LOS), when the receiver gather both the direct and reflecte signals, and Non-Line-of-Sight (NLOS), when the direct signal is not received and only the reflecte signal is gathered. We have previously analyzed the detection of multipath in a quickest detection framework [3]. Notwithstanding, the discrimination between LOS and NLOS was not considered. This discrimination can be very helpful for applying multipath mitigation techniques [4], which are useful when the LOS is present, or decide to apply techniques for exploiting the NLOS multipath such as [5].

Recently, several contributions for distinguishing NLOS from LOS multipath have been proposed. Most of them propose the use of additional hardware like dual-polarized antennas [6], sky plot cameras [7], or map information for performing consistency checks at the measurement level such as in [8]. Nonetheless, the use of external aid is not often available in mass-market GNSS receivers. Furthermore, these detection approaches adopt a framework where time is not explicitly targeted. In order to fulfil the requirements of liability- or safety-critical applications, though, signal integrity should detect the occurrence of a threat as soon as possible.

This work was partly supported by the Spanish Grant TEC2014-53656-R.

For integrity purposes, an acceptable detection delay is limited by a given value m of samples. This kind of detection lies on the fiel of *transient* change detection. In contrast to *quickest* change detection [9], which assumes m to be infinite *transient* change detection deals with finit m. We focus here on non-Bayesian approaches, *i.e.* when the unknown time v at which the change appears is non-random, perfectly fittin the integrity problem. For this framework, the firs optimal results were provided very recently in [10] for the particular case of $m = 1$. For the more general case of f nite $m > 1$, which is the case of signal integrity, the problem is still open. In [11], though, was shown that a Finite Moving Average (FMA) stopping time outperforms other methods available in the literature of transient detection. In this work, we adopt a transient detection framework for discriminating between LOS and NLOS multipath by using the Slope Asymmetry Metric (SAM) -based detection introduced in [3].

Hence, the contribution of this paper is twofold. Firstly, we propose the use of the SAM for LOS and NLOS multipath discrimination. This is motivated by the fact that under LOS a mean change of the SAM prevails, whereas under NLOS conditions a variance change prevails. Secondly, we propose the use of two FMA stopping times, working in parallel, one for detecting a change in the mean of the SAM and another for a change in the variance. This is beneficial as we will show, to obtain simple expressions for theoretical performance bounds. Otherwise, a closed-form expression is not available. Thereby, simple performance bounds are provided and assessed by numerical simulations. Moreover, the outperformance of the proposed solution with respect to the mean and variance change detection in [3] is shown. These are novel contributions since the proposed solution works at the signal processing level, without using additional aid, and adopts a transient change detection framework easily implementable in mass-market GNSS receivers.

The rest of the paper is organized as follows: Section II introduces the signal model for the transient detection based on the SAM metric, Section III presents the proposed method for discriminating LOS and NLOS multipath. Finally, Section IV shows the numerical results, while Section V concludes the paper.

II. Signal Model

The received GNSS signal from the i-th satellite can be modeled as

$$r_i(n) = \eta A s_i(n) + \sum_{k=1}^{N_i} A_{i,k} s_i(n - \tau_{i,k}) e^{j\psi_{i,k}} + w(n), \quad (1)$$

where $s_i(n)$ is the complex base-band signal arriving from the i-th satellite, including any time-delay and Doppler deviations, A is the signal amplitude, N_i is the number of reflecte multipath rays for the i-th satellite, and $\{A_{i,k}, \tau_{i,k}, \psi_{i,k}\}$ are the amplitude, delay (given in samples) and phase of each multipath replica, with $w(n)$ the noise at the receiver. The signal and multipath amplitudes are related by the Signal-to-Multipath Ratio (SMR) as $\mathrm{SMR}_{i,k} = A/A_{i,k}$, and $\eta = \{0, 1\}$ for NLOS and LOS conditions, respectively.

978-1-5090-1757-7/16/$31.00 ©

Let $\{x_n\}_{n\geq 1}$ be an independent and identically distributed (iid) random sequence observed sequentially. We consider a family $\{\mathbb{P}_v | v \in [1, 2, \ldots, \infty]\}$ of probability measures, such that, under $\mathbb{P}_v$, the observations $x_1, \ldots, x_{v-1}$ and $x_{v+m}, \ldots, x_\infty$ are iid with a fixed marginal probability density function (pdf) f_0, with v the deterministic but unknown change time when multipath appears. On the other hand, $x_v, \ldots, x_{v+m-1}$ are iid with another marginal pdf $f_1 \neq f_0$. In this work, we focus on multipath detection relying on the SAM-based detection introduced in [3], modeled herein as

$$x_n \sim \begin{cases} \mathcal{H}_0: & \mathcal{N}(\mu_0, \sigma_0^2) & \text{if } n < v \text{ or } n > v+m \\ \mathcal{H}_1: & \mathcal{N}(\mu_{1,\mathrm{L}}, \sigma_{1,\mathrm{N}}^2) & \text{if } v \leq n \leq v+m \end{cases}, \quad (2)$$

where x_n are the SAM observations, μ_0 and σ_0^2 are the mean and variance of the SAM under normal conditions (i.e. $\mathcal{H}_0$) and $\mu_{1,\mathrm{L}}$, $\sigma_{1,\mathrm{N}}^2$ the mean and variance when LOS (i.e. $\eta = 1$) and NLOS (i.e. $\eta = 0$) multipath is present (i.e. $\mathcal{H}_1$), respectively. Thereby, the appearance of multipath is modeled as a change in the mean and variance of the SAM observations. We assume, without loss of generality, that the acceptable detection delay is equal to the transient change duration m and all parameters are known.

A transient change detection procedure is completely define by its *stopping time* T at which the change is declared, and its performance is measured in terms of the worst-case probability of missed detection and false alarm given by [11]

$$\begin{aligned} \mathbb{P}_{\mathrm{md}}(T) &\doteq \sup_{v\geq 1} \mathbb{P}_v(T \geq v+m-1 | T \geq v), \\ \mathbb{P}_{\mathrm{fa}}(T) &\doteq \sup_{l\geq 1} \mathbb{P}_\infty(l \leq T < l+m_\alpha), \end{aligned} \quad (3)$$

where m_α is the period of samples we want to guarantee $\mathbb{P}_{\mathrm{fa}}$. In this work, we use the FMA stopping time presented in [11], define as

$$T_{\mathrm{MV}} \doteq \inf\{n \geq m : S_n \geq h\}; S_n \doteq \sum_{i=n-m+1}^{n} \mathrm{LLR}_{\mathrm{MV}}(i), \quad (4)$$

with h fixed for assuring a given level of false alarms, and

$$\mathrm{LLR}_{\mathrm{MV}}(n) = a x_n^2 + b x_n + c, \quad (5)$$

with

$$\begin{aligned} a &= \frac{\sigma_{1,\mathrm{N}}^2 - \sigma_0^2}{2\sigma_0^2\sigma_{1,\mathrm{N}}^2}; \quad b = \frac{\sigma_0^2\mu_{1,\mathrm{L}} - \sigma_{1,\mathrm{N}}^2\mu_0}{\sigma_0^2\sigma_{1,\mathrm{N}}^2}; \\ c &= \ln\left(\frac{\sigma_0}{\sigma_{1,\mathrm{N}}}\right) + \frac{\sigma_1^2\mu_0^2 - \sigma_0^2\mu_{1,\mathrm{L}}^2}{2\sigma_0^2\sigma_{1,\mathrm{N}}^2}, \end{aligned} \quad (6)$$

where $\mathrm{LLR}_{\mathrm{MV}}(n) \doteq \ln(f_1(x_n)/f_0(x_n))$ stands for the log-likelihood ratio (LLR) of the observation x_n.

The exact computation of $\mathbb{P}_{\mathrm{md}}$ and $\mathbb{P}_{\mathrm{fa}}$ is difficult, so that the following bounds are used, given in [11],

$$\begin{aligned} \mathbb{P}_{\mathrm{md}}(T_{\mathrm{MV}}) &\leq \beta(h, m), \\ \mathbb{P}_{\mathrm{fa}}(T_{\mathrm{MV}}) &\leq \alpha(h, m_\alpha), \end{aligned} \quad (7)$$

with

$$\begin{aligned} \beta(h, m) &= \mathbb{P}_1(S_m < h) = F_1(h), \\ \alpha(h, m_\alpha) &= 1 - [\mathbb{P}_\infty(S_m < h)]^{m_\alpha} = 1 - [F_0(h)]^{m_\alpha}, \end{aligned} \quad (8)$$

where F_i, with $i = \{0, 1\}$, is the cumulative density function (cdf) of $S_m = \sum_{k=1}^{m} \mathrm{LLR}_{\mathrm{MV}}(k)$ under hypothesis $\mathcal{H}_i$.

III. LOS and NLOS Multipath Discrimination

This section investigates the discrimination between LOS and NLOS multipath, relying on the SAM-based multipath detection. We firstl characterize the SAM under both LOS and NLOS conditions. Secondly, we present the proposed stopping time to detect multipath and to be able to discriminate between LOS and NLOS.

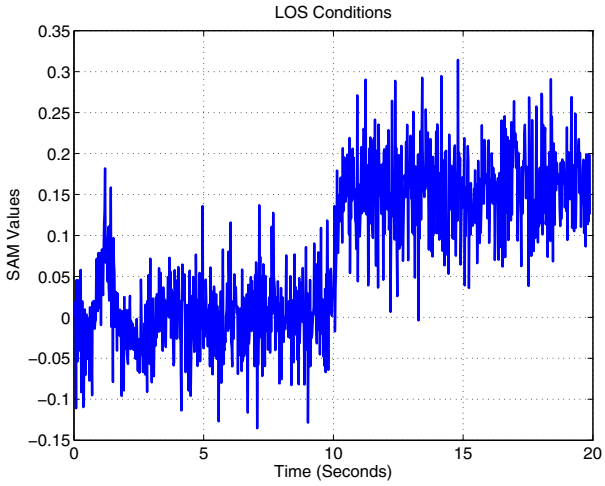

Fig. 1. Simulated SAM for LOS multipath propagation with one ray with SMR = 10dB, $\tau = 0.6$ chips, $\psi = 0$ rad and C/N$_0$= 45 dB-Hz.

A. SAM Characterization Under LOS and NLOS Conditions

The SAM is based on the symmetry of the correlation curves calculated within the GNSS receiver. We know that under $\mathcal{H}_0$ this curve is symmetrical, but it turns to be asymmetrical under $\mathcal{H}_1$. This is measured by the SAM in such a way that it is close to zero under $\mathcal{H}_0$, and it departs from zero under $\mathcal{H}_1$. Specificall , when multipath is present we experience two different effects [12]. That is, under LOS, the mean of the SAM departs from 0, whereas under NLOS the variance of the SAM fluctuates. Indeed, as we stated in [3], in both LOS and NLOS conditions the mean and variance vary, but the mean change is predominant in LOS propagation (i.e. the deterministic component prevails), while the variance change is predominant in NLOS (i.e. random components due to multipath prevails).

In this context, we can clasify the presence of multipath (i.e. $\mathcal{H}_1$) into two different hypotheses, $\mathcal{H}_{\mathrm{L}}$ and $\mathcal{H}_{\mathrm{N}}$ for LOS and NLOS conditions, respectively, as follows

$$x_n \sim \begin{cases} \mathcal{H}_0: & \mathcal{N}(\mu_0, \sigma_0^2) & \text{if } n < v \text{ or } n > v+m \\ \mathcal{H}_{\mathrm{L}}: & \mathcal{N}(\mu_{1,\mathrm{L}}, \sigma_0^2) & \text{if LOS multipath} \\ \mathcal{H}_{\mathrm{N}}: & \mathcal{N}(\mu_0, \sigma_{1,\mathrm{N}}^2) & \text{if NLOS multipath} \end{cases}. \quad (9)$$

Based on the previous idea, we can discriminate between LOS and NLOS identifying whether the mean or variance change in the SAM is prevalent, respectively. For instance, for the LOS case, we see in Fig. 1 how the mean change prevails. Indeed, we see a mean change but the variance is similar. This result is obtained by simulating an static GNSS receiver with a multipath ray appearing at second 10 with SMR = 10 dB, $\tau = 0.6$ chips, $\psi = 0$ rad, and a carrier-to-noise ratio (C/N$_0$) of 45 dB-Hz (tentative values in urban environments).

Thereby, we can write the following model for the LOS situation

$$x_{n,\mathrm{L}} \sim \begin{cases} \mathcal{H}_0: & \mathcal{N}(\mu_0, \sigma_0^2) & \text{if } n < v \text{ or } n > v+m \\ \mathcal{H}_{\mathrm{L}}: & \mathcal{N}(\mu_{1,\mathrm{L}}, \sigma_0^2) & \text{if } v \leq n \leq v+m \end{cases}, \quad (10)$$

where $x_{n,\mathrm{L}}$ and $\mu_{1,\mathrm{L}}$ are the SAM metric observations and mean when LOS multipath is present. That is, we model LOS conditions as a mean change of the SAM. So, we have the following LLR

$$\mathrm{LLR}_{\mathrm{M}}(n) = \frac{\mu_{1,\mathrm{L}} - \mu_0}{\sigma_0^2}\left(x_{n,\mathrm{L}} - \frac{\mu_{1,\mathrm{L}} + \mu_0}{2}\right), \quad (11)$$

leading to the following bounds for the probability of missed detec-

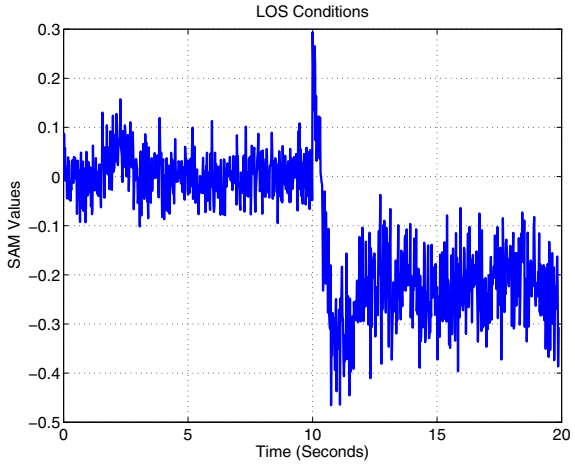

Fig. 2. Simulated SAM for a LOS multipath propagation with one ray with SMR $= 10$ dB, $\tau = 0.3$ chips, $\psi = \pi$ rad and C/N$_0$= 45 dB-Hz.

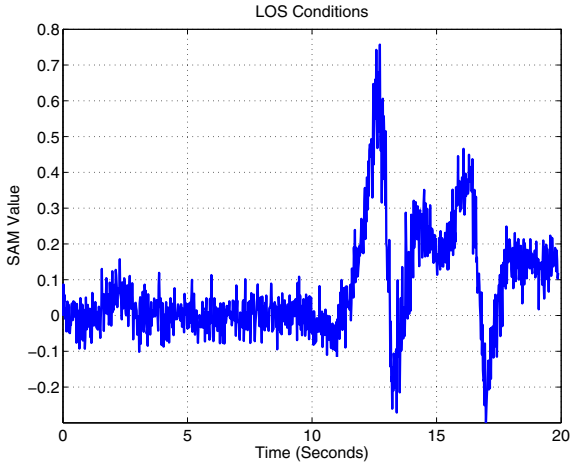

Fig. 3. Simulated SAM for a LOS multipath propagation with three rays with SMR $= \{5, 10, 7\}$ dB, $\tau = \{0.3, 0.7, 0.4\}$ chips, $\psi = \{0, \pi, \pi/2\}$ rad, C/N$_0$= 45 dB-Hz and Doppler frequency $f_{\rm d} = 1.38 \cdot c \cdot \tau \cdot t_{\rm ch}$ mHz, where $c = 3e8$ m/s and $t_{\rm ch} = 0.9775$ μs.

tion and false alarms [11]

$$\beta_{\rm M}\left(h, m\right) = \Phi\left(\frac{h - m\mu_{\rm M}}{\sqrt{m\sigma^2_{\rm M}}}\right), \tag{12}$$

$$\alpha_{\rm M}\left(h, m_\alpha\right) = 1 - \left[\Phi\left(\frac{h + m\mu_{\rm M}}{\sqrt{m\sigma^2_{\rm M}}}\right)\right]^{m_\alpha}, \tag{13}$$

with $\Phi(x)$ the standard normal cdf evaluated at x, and

$$\begin{aligned} \mu_{\rm M} &= \frac{\left(\mu_{1,{\rm L}} - \mu_0\right)^2}{2\sigma_0^2}, \\ \sigma^2_{\rm M} &= 2\mu_{\rm M}. \end{aligned} \tag{14}$$

We have seen from Fig. 1 that no change in the variance is present. However, there may be situations where the variance may slightly vary when LOS multipath is present. This is shown in Fig. 2 where we simulate a LOS multipath ray appearing at second 10, with the following parameters: SMR $= 10$ dB, $\tau = 0.3$ chips, $\psi = \pi$ rad, and C/N$_0$= 45 dB-Hz (also tentative). We see how in this case, in addition to the mean change, the variance of the SAM slightly increases. Notwithstanding, we see how the mean change is prevalent, so that (10) is still valid. Similar results are obtained, as it is shown in Fig. 3, with a more realistic simulation with three multipath rays appearing at second 10 and SMR $= \{5, 10, 7\}$ dB, $\tau = \{0.3, 0.7, 0.4\}$ chips, $\psi = \{0, \pi, \pi/2\}$ rad, C/N$_0$= 45 dB-Hz and a Doppler frequency $f_{\rm d} = 1.38 \cdot c \cdot \tau \cdot t_{\rm ch}$ mHz, where $c = 3e8$ m/s and $t_{\rm ch} = 0.9775$ μs, simulating the movement of the satellite as in [13].

On the other hand, we present in Fig. 4 the results obtained by simulating a moving receiver approaching the reflecto with a NLOS multipath ray appearing at second 10 with the following parameters: SMR $=$ 20–5dB, $\tau = 0.7$–0.3 chips, $\psi = 0$–π rad, and C/N$_0$= 45 dB-Hz. We see how the variance of the SAM increases abruptly just when the multipath appears, and then it decreases as the receiver is approaching the reflecto . Regarding the mean of the SAM, it remains constant along the whole simulation. Similarly as for the LOS case, there may be situations where the mean of the SAM slightly varies under NLOS conditions, but the change in the variance will prevail.

Hence, we can conclude that under NLOS situation, the SAM experiences a change in the variance, and thus we can write

$$x_{n,{\rm N}} \sim \begin{cases} \mathcal{H}_0: & \mathcal{N}(\mu_0, \sigma_0^2) & \text{if } n < v \text{ or } n > v + m \\ \mathcal{H}_{\rm N}: & \mathcal{N}(\mu_0, \sigma_{1,{\rm N}}^2) & \text{if } v \le n \le v + m \end{cases}, \tag{15}$$

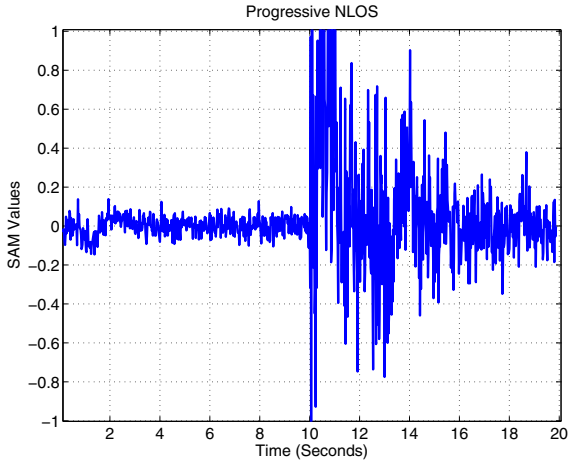

Fig. 4. SAM for a NLOS multipath propagation simulating a moving receiver approaching the reflecto with the following varying multipath parameters: SMR $=$ 20–5dB, $\tau = 0.7$–0.3 chips, $\psi = 0$–π rad, and C/N$_0$= 45 dB-Hz.

where $x_{n,{\rm N}}$ and $\sigma^2_{1,{\rm N}}$ stand for the SAM observations and variance when NLOS multipath is present. Thereby, we have

$$\text{LLR}_{\rm V}(n) = \gamma x^2_{n,{\rm N}} + \delta, \tag{16}$$

with

$$\begin{aligned} \gamma &= \frac{\sigma^2_{1,{\rm N}} - \sigma_0^2}{2\sigma_0^2\sigma^2_{1,{\rm N}}}, \\ \delta &= \ln\left(\frac{\sigma_0}{\sigma_{1,{\rm N}}}\right), \end{aligned} \tag{17}$$

leading, from (7) and after simple manipulations, to

$$\beta_{\rm V}\left(h, m\right) = \Gamma_m\left(\frac{h - m\delta}{k_1}\right), \tag{18}$$

$$\alpha_{\rm V}\left(h, m_\alpha\right) = 1 - \left[\Gamma_m\left(\frac{h - m\delta}{k_0}\right)\right]^{m_\alpha}, \tag{19}$$

where $\Gamma_m(x)$ denotes the cdf of the chi-squared distribution with m degrees of freedom, $k_1 = \sigma^2_{1,{\rm N}}\gamma$ and $k_0 = \sigma_0^2\gamma$.

B. Parallel FMA Stopping Time

Here, based on the previous results, we propose the use of two different stopping times, working in parallel, one for detecting a change in the mean of the SAM and another for the variance. Thereby, we will detect multipath whenever one of the stopping times declares so, and we will be able to discriminate between LOS or NLOS when the change in the mean or variance is declared, respectively. To do so, we defin

$$\begin{aligned} T_{\mathrm{P}} &\doteq \inf\left\{n \geq m : \{S_{n,\mathrm{M}} \geq h_{\mathrm{M}}\} \text{ or } \{S_{n,\mathrm{V}} \geq h_{\mathrm{V}}\}\right\} \\ &= \min\left\{T_{\mathrm{M}}, T_{\mathrm{V}}\right\}, \end{aligned} \tag{20}$$

where T_{M} (h_{M}) and T_{V} (h_{V}) are the stopping times (detection thresholds) for detecting a change in the mean and variance, respectively, define as

$$\begin{aligned} T_{\mathrm{M}} &\doteq \inf\left\{n \geq m : S_{n,\mathrm{M}} \geq h_{\mathrm{M}}\right\}, \\ T_{\mathrm{V}} &\doteq \inf\left\{n \geq m : S_{n,\mathrm{V}} \geq h_{\mathrm{V}}\right\}, \end{aligned} \tag{21}$$

with

$$\begin{aligned} S_{n,\mathrm{M}} &\doteq \sum_{i=n-m+1}^{n} \mathrm{LLR}_{\mathrm{M}}(i), \\ S_{n,\mathrm{V}} &\doteq \sum_{i=n-m+1}^{n} \mathrm{LLR}_{\mathrm{V}}(i), \end{aligned} \tag{22}$$

and $\{\mathrm{LLR}_{\mathrm{M}}, \mathrm{LLR}_{\mathrm{V}}\}$ given by (11) and (16), respectively. Thereby, from (3) and the definitio of T_{P} in (20), we have

$$\begin{aligned} \mathbb{P}_{\mathrm{md}}\left(T_{\mathrm{P}}\right) &\doteq \sup_{v>m} \mathbb{P}_v\left(T_{\mathrm{P}} \geq v+m-1 | T_{\mathrm{P}} \geq v\right) \\ &\leq \min\left\{\mathbb{P}_{\mathrm{md}}\left(T_{\mathrm{M}}\right), \mathbb{P}_{\mathrm{md}}\left(T_{\mathrm{V}}\right)\right\}, \end{aligned} \tag{23}$$

where the inequality follows because despite T_{M} detected faster than T_{V} on average, there might be realizations in which T_{V} detects faster, or viceversa. Similarly, for $\mathbb{P}_{\mathrm{fa}}$ we have

$$\begin{aligned} \mathbb{P}_{\mathrm{fa}}\left(T_{\mathrm{P}}\right) &\doteq \sup_{l \geq m} \mathbb{P}_{\infty}\left(l \leq T_{\mathrm{P}} < l + m_{\alpha}\right) \\ &\geq \max\left\{\mathbb{P}_{\mathrm{fa}}\left(T_{\mathrm{M}}\right), \mathbb{P}_{\mathrm{fa}}\left(T_{\mathrm{V}}\right)\right\}. \end{aligned} \tag{24}$$

Therefore, since both T_{M} and T_{V} are FMA stopping times they fulfil the bounds in (7), and then

$$\beta_{\mathrm{p,L}}\left(h_{\mathrm{M}}, h_{\mathrm{V}}, m\right) = \min\left\{\beta_{\mathrm{M}}\left(h_{\mathrm{M}}, m\right), \beta_{\mathrm{V,L}}\left(h_{\mathrm{V}}, m\right)\right\}, \tag{25}$$

$$\beta_{\mathrm{p,N}}\left(h_{\mathrm{M}}, h_{\mathrm{V}}, m\right) = \min\left\{\beta_{\mathrm{M,N}}\left(h_{\mathrm{M}}, m\right), \beta_{\mathrm{V}}\left(h_{\mathrm{V}}, m\right)\right\}, \tag{26}$$

with $\beta_{\mathrm{p,L}}$ and $\beta_{\mathrm{p,N}}$ the upper bound for $\mathbb{P}_{\mathrm{md}}(T_{\mathrm{P}})$ under LOS and NLOS conditions, respectively, $\{\beta_{\mathrm{M}}, \beta_{\mathrm{V}}\}$ given by (12) and (18), respectively, and $\{\beta_{\mathrm{M,N}}, \beta_{\mathrm{V,L}}\}$ the upper-bound for $\mathbb{P}_{\mathrm{md}}(T_{\mathrm{M}})$ and $\mathbb{P}_{\mathrm{md}}(T_{\mathrm{V}})$ under NLOS and LOS conditions, respectively, given by

$$\beta_{\mathrm{M,N}}\left(h_{\mathrm{M}}, m\right) = \Phi\left(\frac{h_{\mathrm{M}} + m\mu_{\mathrm{M}}}{\sqrt{m}\tilde{\sigma}}\right), \tag{27}$$

$$\beta_{\mathrm{V,L}}\left(h_{\mathrm{V}}, m\right) = \Gamma_m\left(\frac{h_{\mathrm{V}} - m\delta}{k_0}; \lambda\right), \tag{28}$$

with $\tilde{\sigma}^2 = \sigma_{\mathrm{M}}^2(\sigma_{1,\mathrm{N}}^2/\sigma_0^2)$ and $\Gamma_m(x;\lambda)$ the cdf of the non-central chi-squared distribution with non-central parameter $\lambda = m(\mu_{1,\mathrm{L}}^2/\sigma_0)$. Similarly, $\mathbb{P}_{\mathrm{fa}}(T_{\mathrm{P}})$ is upper-bounded by

$$\alpha_{\mathrm{p}}\left(h_{\mathrm{M}}, h_{\mathrm{V}}, m_{\alpha}\right) = \max\left\{\alpha_{\mathrm{M}}\left(h_{\mathrm{M}}, m_{\alpha}\right), \alpha_{\mathrm{V}}\left(h_{\mathrm{V}}, m_{\alpha}\right)\right\}, \tag{29}$$

since the bounds α_{M} and α_{V} are the same in both LOS and NLOS cases. Nevertheless, from (24) we have a lower-bound, and then this result will be only true when the change in the mean or variance is much greater than the other, which is our case for the SAM, and then (24) turns out to be an equality.

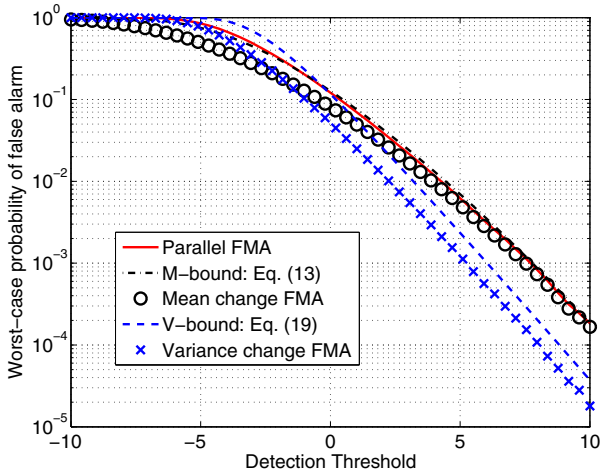

Fig. 5. Numerical simulations of the probability of false alarm $\mathbb{P}_{\mathrm{fa}}(T)$ for the parallel, mean and variance change stopping times, with their respective bounds in (13) and (19).

Finally, it is worth mentioning that the main interest for using the parallel stopping time presented in (20) is due to the discrimination between LOS and NLOS multipath detection. Nonetheless, it is also motivated by the fact that the bounds for $\mathbb{P}_{\mathrm{md}}$ and $\mathbb{P}_{\mathrm{fa}}$ in (7) for T_{MV} are complicated to obtain in a closed-form. This is because for T_{MV}, we should obtain the distribution of the summation of a non-central chi-squared and Gaussian random variables (see (5)), which is not a trivial problem. Notwithstanding, the bounds for T_{M} and T_{V} in (21), previously obtained, can be easily computed from the standard Gaussian and chi-squared cdfs. Therefore, the use of the parallel stopping time also extremely reduces the complexity for computing the performance bounds.

IV. Numerical Results

The goal of this section is to frstly asses the goodness of the theoretical bounds in Section III by making use of numerical simulations. Secondly, the proposed parallel stopping time T_{P} in (20) is compared with the stopping time for detecting a change in both the mean and variance of the SAM T_{MV} in (4) and the stopping times for detecting a change in either the mean or variance of the SAM T_{M} or T_{V} in (21). All the simulation parameters used for the SAM are motivated by the obtained results in Section III.

A. CASE1: Goodness of performance bounds

Here, we assess the goodness of the theoretical bounds, proposed in Section III, with numerical simulations of the worst-case probability of missed detection $\mathbb{P}_{\mathrm{md}}(T)$ and false alarm for a given duration m_{α}, $\mathbb{P}_{\mathrm{fa}}(T)$. We fx $h_{\mathrm{M}} = h_{\mathrm{V}} = h$ so that we can compare T_{M}, T_{V} and T_{P} with a common threshold. Fig. 5 shows $\mathbb{P}_{\mathrm{fa}}$ as a function of the detection threshold h. This probability is compared with the bounds for T_{M}, T_{V} and T_{P} given by (13), (19) and (29), respectively. We use the following parameters: $\mu_0 = 0$, $\mu_{1,\mathrm{L}} = 0.15$, $\sigma_0^2 = 5e-3$ and $\sigma_{1,\mathrm{N}}^2 = 17\sigma_0^2$. We see how the proposed bound for $\mathbb{P}_{\mathrm{fa}}$ is fulfille with all the stopping times. Indeed, we see how for small values of threshold h, $\mathbb{P}_{\mathrm{fa}}(T_{\mathrm{V}})$ is greater than $\mathbb{P}_{\mathrm{fa}}(T_{\mathrm{M}})$, and then the upper-bound for the parallel stopping time T_{P} is given by the bound for T_{V} in (19). On the other hand, for big h, T_{M} gives worse $\mathbb{P}_{\mathrm{fa}}$, so that the bound for T_{P} is given by the bound for T_{M} in (13).

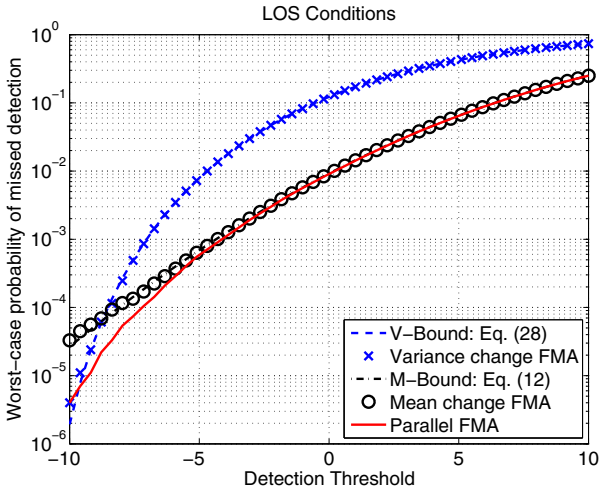

Fig. 6. Numerical simulations of the probability of missed detection $\mathbb{P}_{\rm md}(T)$ for the considered stopping times under LOS conditions, with their respective bounds in (12) and (28).

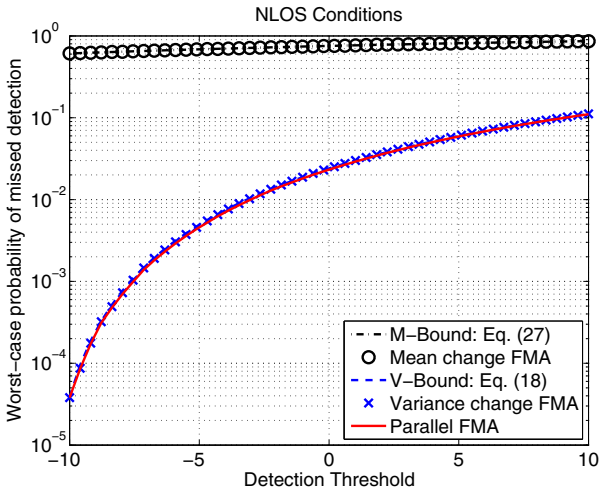

Fig. 7. Numerical simulations of $\mathbb{P}_{\rm md}(T)$ for the considered stopping times under NLOS conditions, with their respective bounds in (27) and (18).

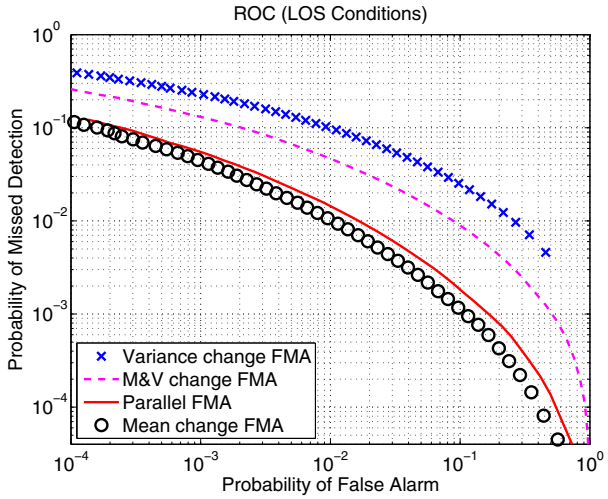

Fig. 8. ROC under LOS conditions for the analyzed stopping times with $\mu_0 = 0$, $\mu_{1,\rm L} = 0.15$, $\sigma_0^2 = 4e-3$ and $\sigma_{1,\rm N}^2 = 12\sigma_0^2$.

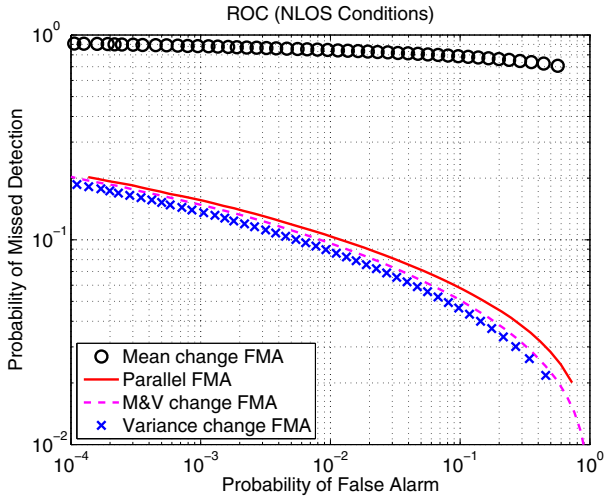

Fig. 9. ROC under NLOS conditions for the analyzed stopping times with $\mu_0 = 0$, $\mu_{1,\rm L} = 0.15$, $\sigma_0^2 = 4e-3$ and $\sigma_{1,\rm N}^2 = 12\sigma_0^2$.

Similar results are obtained for $\mathbb{P}_{\rm md}$, under LOS conditions, in Fig. 6. That is, for small h, $T_{\rm V}$ gives better $\mathbb{P}_{\rm md}$, and then $\mathbb{P}_{\rm md}(T_{\rm P})$ is upper-bounded by the bound for $T_{\rm V}$ in (28). For big h, $T_{\rm M}$ provides the lowest $\mathbb{P}_{\rm md}$, and then the bound for $T_{\rm P}$ is given by the bound for $T_{\rm M}$ in (12). Finally, Fig. 7 shows $\mathbb{P}_{\rm md}$ for the case of NLOS conditions. We see how in this case the $T_{\rm V}$ always gives the best results, in terms of missed detection, and then the bound for the parallel stopping time is given by the bound for $T_{\rm V}$ in (18).

B. CASE2: ROC Comparison

Now, we compare $T_{\rm P}$, in terms of $\mathbb{P}_{\rm md}$ as a function of $\mathbb{P}_{\rm fa}$, henceforth referred as to the Receiver Operating Characteristic (ROC), with $T_{\rm MV}$, $T_{\rm M}$ and $T_{\rm V}$. For computing the ROC, we fi $h_{\rm M}$ and $h_{\rm V}$ from (13) and (16), respectively, as

$$\begin{aligned} h_{\rm M} &= \sqrt{m\sigma_{\rm M}^2}\Phi\left((1-\alpha)^{1/m_\alpha}\right) - m\mu_{\rm M}, \\ h_{\rm V} &= k_0\Gamma_m\left((1-\alpha)^{1/m_\alpha}\right) + m\delta, \end{aligned} \tag{30}$$

with α taking values from 10^{-4} to 1. Then, we numerically obtain $\mathbb{P}_{\rm md}$ and $\mathbb{P}_{\rm fa}$ with 10^6 Monte-Carlo runs. Fig. 8 and Fig. 9 show the ROC for each analyzed stopping time for LOS and NLOS conditions, respectively, with the following parameters: $\mu_0 = 0$, $\mu_{1,\rm L} = 0.15$, $\sigma_0^2 = 4e-3$ and $\sigma_{1,\rm N}^2 = 12\sigma_0^2$.

We see in Fig. 8 how for the LOS case $T_{\rm P}$ outperforms $T_{\rm MV}$. This is because there is not change in variance, and then the model used for $T_{\rm MV}$ is not actually true, hindering the detection. Meanwhile, $T_{\rm P}$ approaches $T_{\rm M}$, which provides the best results in terms of ROC. Furthermore, we see in Fig. 9 that for the NLOS case, the $T_{\rm MV}$ slightly outperforms the parallel stopping time. In this case, the difference in terms of performance between $T_{\rm M}$ and $T_{\rm V}$ is huge, and then $T_{\rm P}$ is badly affected by the poor performance of $T_{\rm M}$, whereas for $T_{\rm MV}$ this difference make it to approach $T_{\rm V}$, which produce the best results in terms of ROC.

In order to consider those cases where the variance under LOS conditions vary, on the one hand we show in Fig. 10 the results for the ROC with: $\mu_0 = 0$, $\mu_{1,\rm L} = 0.2$, $\sigma_0^2 = 4e-3$, $\sigma_{1,\rm N}^2 = 12\sigma_0^2$

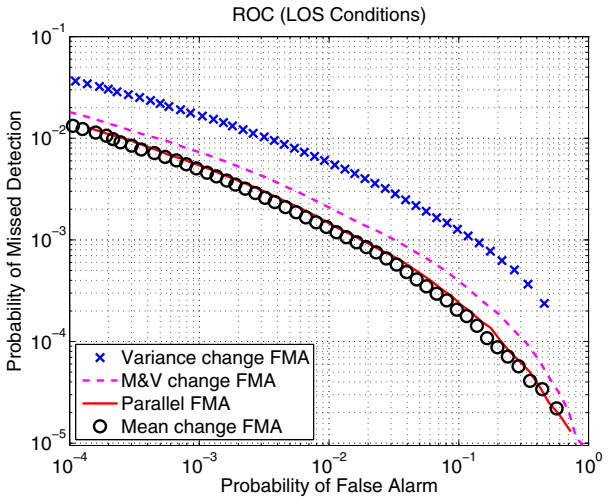

Fig. 10. ROC under LOS conditions for the analyzed stopping times with $\mu_0 = 0$, $\mu_{1,\mathrm{L}} = 0.2$, $\sigma_0^2 = 4e-3$, $\sigma_{1,\mathrm{N}}^2 = 12\sigma_0^2$ and $\sigma_{1,\mathrm{L}}^2 = 2\sigma_0^2$.

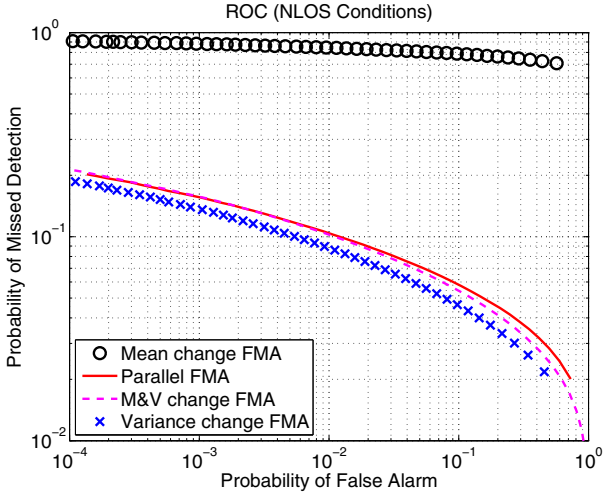

Fig. 11. ROC under NLOS conditions for the analyzed stopping times with $\mu_0 = 0$, $\mu_{1,\mathrm{L}} = 0.2$, $\sigma_0^2 = 4e-3$, $\sigma_{1,\mathrm{N}}^2 = 12\sigma_0^2$ and $\sigma_{1,\mathrm{L}}^2 = 2\sigma_0^2$.

and $\sigma_{1,\mathrm{L}}^2 = 2\sigma_0^2$, with $\sigma_{1,\mathrm{L}}^2$ the variance under LOS multipath (i.e. σ_0^2 in (10)). We see that T_{P} still outperforms T_{MV}, but slightly less than previously. This is so because we have included a change in the variance and then the T_{MV} is benefited but not enough as for outperforming T_{P}. On the other hand, in Fig. 11, we see that for the NLOS case both T_{P} and T_{MV} provides similar performance. It is worth noting that the parameters used for these simulations are intended to provide qualitative results. In practice, the cases where the variance vary under LOS conditions is linked with a change in the mean greater than that simulated (see Fig. 2). Hence, in practice, under LOS conditions the difference between T_{P} and T_{MV} will be greater, and then T_{P} will still outperform even with larger changes in the variance.

V. Conclusions

This paper has investigated the problem of discriminating between LOS and NLOS multipath conditions in GNSS receivers. To do so, we have proposed a novel transient change detection framework by using two FMA stopping times, one for detecting a mean change and another for a variance change of the SAM. This is motivated by the fact that the SAM experiences a mean change under LOS conditions, whereas it experiences a variance change under NLOS conditions, which has been shown by realistic simulations. Theoretical bounds for the probability of missed detection and false alarm for the considered stopping times have been proposed and numerically assessed. Moreover, we have compared with numerical simulations the performance in terms of ROC of the considered stopping times for different scenarios of practical interest. These simulations have confirme the outperformance of the proposed solution, with respect to the solution for detecting a change in both the mean and variance of the SAM. Therefore, the use of the proposed solution may benefi those applications where the discrimination between LOS and NLOS multipath is of interest, such as GNSS integrity, drastically reducing the complexity for computing the performance bounds, which is a key factor in integrity algorithms. Otherwise we should use the stopping time for detecting both changes in the mean and variance, which has not a trivial expression for the performance bounds. Moreover, the proposed solution does not rely on external aid, which is a novel aspect since so far the contributions for discimiating between LOS and NLOS conditons make use of some external aid, which is not often available in mass-market GNSS receivers.

References

[1] G. Seco-Granados, J. A. López-Salcedo, D. Jiménez-Baños, and G. López-Risueño, "Challenges in Indoor Global Navigation Satellite Systems: Unveiling its core features in signal processing," *IEEE Signal Processing Magazine*, vol. 29, no. 2, pp. 108–131, 2012.

[2] J. Cosmen-Schortmann, M. Azaola-Saenz, M. Martínez-Olagüe, and M. Toledo-Lopez, "Integrity in urban and road environments and its use in liability critical applications," in *IEEE/ION Position, Location and Navigation Symposium*, 2008, pp. 972–983.

[3] D. Egea-Roca *et al.*, "Signal-level Integrity and Metrics Based on the Application of Quickest Detection Theory to Multipath Detection," in *ION GNSS+*, 2015, pp. 2926–2938.

[4] M. Z. H. Bhuiyan, E. S. Lohan, and M. Renfors, "Code tracking algorithms for mitigating multipath effects in fading channels for satellite-based positioning," *EURASIP Journal on Advances in Signal Processing*, vol. 2008, no. 1, pp. 1–17, 2007.

[5] C. Genter, R. Phlmann, M. Ulmschneider, T. Jost, and A. Dammann, "Multipath Assisted Positioning for Pedestrians," in *ION GNSS+*, 2015, pp. 2079–2086.

[6] P. Groves, Z. Jiang, B. Skelton, P. Cross, L. Lau, Y. Adane, and I. Kale, "Novel Multipath Mitigation Methods using a Dual-Polarization Antenna," in *ION GNSS+*, 2010, pp. 140–151.

[7] E. Shytermeja, A. Garcia-Pena, and O. Julien, "Proposed architecture for integrity monitoring of a GNSS/MEMS system with a Fisheye camera in urban environment," in *ICL-GNSS*, 2014, pp. 1–6.

[8] L. T. Hsu and S. Kamijo, "NLOS Exclusion using Consistency Check and City Building Model in Deep Urban Canyons," in *ION GNSS+*, 2015, pp. 2390–2396.

[9] H. V. Poor and O. Hadjiliadis, *Quickest Detection*. Cambridge University Press, 2009.

[10] G. V. Moustakides, "Multiple Optimality Properties of the Shewhart Test," *Sequential Analysis*, vol. 33, pp. 318–344, 2014.

[11] D. Egea-Roca, G. Seco-Granados, J. A. López-Salcedo, and H. V. Poor, "A Finite Moving Average Test for Transient Change Detection in GNSS Signal Strength Monitoring," in *IEEE SSP*, 2016.

[12] J. A. López-Salcedo, J. M. Parro-Jiménez, and G. Seco-Granados, "Multipath detection metrics and attenuation analysis using a GPS snapshot receiver in harsh environments," in *IEEE EuCAP*, 2009, pp. 3692–3696.

[13] R. D. J. Van Nee, "Multipath effects on GPS code phase measurements," *Navigation*, vol. 39, no. 2, pp. 177–190, 1992.